

CHAPTER 55

Biperiodic Waves in Shallow Water

Norman W. Scheffner*, Member ASCE

Introduction

The propagation of waves in shallow water is a phenomenon of significant practical importance. The ability to realistically predict the complex wave characteristics occurring in shallow water regions has always been an engineering goal which would make the development of solutions to practical engineering problems a reality. The difficulty in making such predictions stems from the fact that the equations governing the complex three-dimensional flow regime can not be solved without linearizing the problem. The linear equations are solvable; however, their solutions do not reflect the nonlinear features of naturally occurring waves. A recent advance (1984) in nonlinear mathematics has resulted in an explicit solution to a nonlinear equation relevant to water waves in shallow water. This solution possesses features found in observed nonlinear three-dimensional wave fields.

The nonlinear mathematical formulation referred to above has never been compared with actual waves, so that its practical value is unknown. The purpose of the present investigation was to physically generate three-dimensional nonlinear waves and compare these with exact mathematical solutions. The goals were successfully completed by first generating the necessary wave patterns with the new U.S. Army Engineer Waterways Experiment Station, Coastal Engineering Research Center's (CERC) directional spectral wave generation facility. The theoretical solutions were then formed through the determination of a unique correspondence between the free parameters of the solution and the physical characteristics of the generated wave.

*Research Hydraulic Engineer, U.S. Army Engineer Waterways Experiment Station, Coastal Engineering Research Center, Vicksburg, Mississippi, USA

Theoretical Background

One of the first mathematical models of nonlinear waves in shallow water with known solutions was presented by Korteweg and deVries in their famous 1895 paper. Their model, known as the KdV equation can be written in the following nondimensional form

$$f_t + 6ff_x + f_{xxx} = 0 \quad (1)$$

in which f represents the water surface displacement, x is the direction of wave propagation and t is time. This equation admits not only solitary wave solutions but also the periodic solutions commonly known as cnoidal waves. These solutions can be written as

$$f(x,t) = 2\sigma^2 k^2 \text{cn}^2(\theta; k) - 2\sigma^2 \left[\frac{E(k)}{K(k)} - 1 + k^2 \right] \quad (2)$$

where each of the terms in the solution are well documented analytic functions which can easily be computed in terms of known wave characteristics such as wave height and wavelength. Unfortunately, cnoidal wave solutions are valid only for long crested waves, e.g., waves which can be described by a single time-dependent one-dimensional surface wave pattern. Natural waves, in contrast, are composed of both long and short crested waves and cannot be adequately described by this theory.

A recent advance in nonlinear mathematics has been reported by Segur and Finkel (1984). They present explicit analytical solutions to a natural three-dimensional extension of the KdV equation proposed by Kadomtsev and Petviashvili (1970), known as the KP equation shown below

$$\left(f_x + 6ff_x + f_{xxx} \right)_x + 3f_{yy} = 0 \quad (3)$$

where x now represents the primary direction of propagation; however, weak changes in the y -direction are now permitted. When no y -variations occur, the KP equation reverts to the KdV equation.

The KP equation admits an infinitely dimensional family of exact, periodic, solutions (see Dubrovin 1981 and Segur and Finkel 1984) which can be written in the form

$$f(x, y, t) = 2 \frac{\partial^2 \ln \theta}{\partial x^2} \quad (4)$$

where θ is a Riemann theta function of genus n . Genus 1 solutions are exactly equivalent to cnoidal waves, they are permanent form, singly periodic, two-dimensional (one vertical and one horizontal) nonlinear waves. Genus 2 waves are biperiodic in that they permit the independent specification of two periodicities in both time and space. The solutions are genuinely three-dimensional, nonlinear, and propagate with permanent form at a constant velocity. Genus 3 and higher order solutions are multi-periodic and cannot be characterized as permanent form with respect to any translating coordinate system as the genus 1 and 2 solutions can. This present investigation is limited to the genus 2 solutions developed by Segur and Finkel.

The construction of a genus 2 solution of the KP equation is based on the specification of the appropriate Riemann theta function. This requires the introduction of a two-component phase variable and a 2×2 real-valued Riemann matrix. The first of these, the phase variable, is shown below.

$$\begin{aligned} \phi_1 &= \mu_1 x + \nu_1 y + \omega_1 t + \phi_{10} \\ \text{and} \\ \phi_2 &= \mu_2 x + \nu_2 y + \omega_2 t + \phi_{20} \end{aligned} \quad (5)$$

Where the parameters μ_1 , μ_2 , ν_1 , and ν_2 are wave numbers, ω_1 , and ω_2 are angular frequencies, and ϕ_{10} and ϕ_{20} are constants with no dynamical significance. The second ingredient involves the specification of a real-valued, negative definite, symmetric 2×2 Riemann matrix as shown below.

$$B = \begin{pmatrix} b & b\lambda \\ b\lambda & b\lambda^2 + d \end{pmatrix} \quad (6)$$

The parameters b , d , and λ represent solution non-linearity. The genus 2 theta function can now be defined in terms of the above components by the following double Fourier series:

$$\theta(\phi_1, \phi_2, B) = \sum_{m_1=-\infty}^{\infty} \sum_{m_2=-\infty}^{\infty} \exp\left(\frac{1}{2} m \cdot B \cdot m + i m \cdot \phi\right) \quad (7)$$

The calculation of a general case genus 2 KP solution requires the specification of the 11 parameters shown in Equations 5 and 6. Two of these parameters (ϕ_{10} and ϕ_{20}) have no dynamical significance, their only effect is to shift the origin of the resulting solution. Dubrovin (1981) proved that a genus 2 theta function in

the form of Equation 7 was a solution to the KP equation if, and only if, the solution parameters were related by four additional equations. One of these equations contains a constant of integration. Use of this additional criteria reduces the number of free parameters to 8, representing the minimum number of free parameters required to specify a general case genus 2 solution.

Genus 2 solutions of the KP equation describe a complex two-dimensional surface wave pattern. Similar features were observed by Hammack (1980) to result from the nonlinear interaction of two intersecting waves. The theoretical development by Segur and Finkel was partially prompted, in fact, by these reported waves. The development of an experimental program which would result in the generation of surface wave patterns qualitatively similar to genus 2 solutions was achieved by attempting to experimentally reproduce the conditions reported by Hammack, i.e. intersecting waves. This generation technique can best be described by presenting the analogy of interacting waves. Consider, for example, two periodic waves which intersect and pass through each other as shown in Figure 1. The angles α_1 and α_2 represent the angle of the crest of each wave front with respect to some reference line. The resulting surface wave pattern, according to linear wave theory, would simply be a superposition of the two individual waves. This would produce a diamond shaped surface pattern as indicated in Figure 1. It can be seen that certain of the basic characteristics of the individual waves, wavelength and angle of propagation for example, have been preserved.

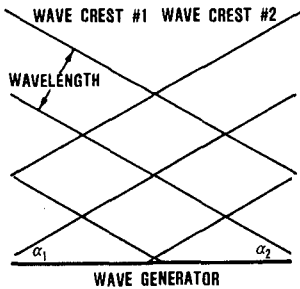


Figure 1. The Linear Intersection of Waves

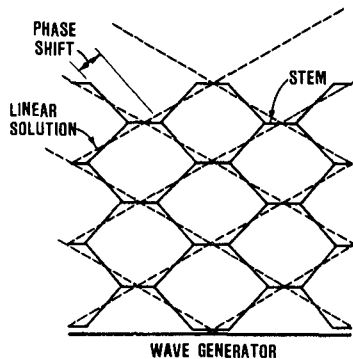


Figure 2. The Nonlinear Intersection of Waves

Now, consider the analogous case in which similarly intersecting waves interact nonlinearly with each other. This scenario is shown schematically in Figure 2. The resulting wave pattern shows that a "stem of interaction" is formed at the point where the two waves

cross each other. The formation of this stem region is a result of a phase shift in the crest line angles of the original waves. This phenomenon is shown in Figure 2 superimposed on the corresponding linear wave solution. The resulting surface wave pattern now assumes a hexagonal pattern in which a third wave crest, separate of the original two, is formed. This phase shift and stem formation are indicative of the nonlinear interaction of the two waves since the exact linear solution does not predict either the phase shift or the new wave crest. Genus 2 solutions of the KP equation predict these features and was tested as a possible model for their description.

Laboratory Facilities and Experimental Procedures

A project was initiated at CERC to generate three-dimensional nonlinear wave fields in the laboratory and then to apply KP theory to the resulting waves in order to determine whether or not the KP equation was a model for these waves and, if so, what was the range of its applicability. This required the use of the CERC directional spectral wave generation facility. This unique wave generator, shown in Figure 3, was designed and constructed for CERC by MTS Systems Corporation of Minneapolis, Minnesota, based on design specifications provided by CERC. The generator is comprised of 60 individually programmable electromechanical wave paddles. Each wave paddle is 1.5 ft wide making the generator a total of 90.0 ft in width. The generator is located in a 98.0 by 184.0-ft wave basin with 2.5 ft high side walls. Computer control of the system is provided by a Digital Equipment Corporation (DEC) VAX 11/750 central processing unit. The above facilities were utilized to generate genus 2 candidate waves in a comprehensive experimental program.



Figure 3. The Directional Spectral Wave Generator

The wave generator was programmed to simultaneously generate intersecting cnoidal wave trains. A variety of wave fields were generated by varying both the wavelength of the individual waves and their angle of intersection. Twelve wave fields, generated in this manner, were used to test the KP equation. The wave fields selected for the experimental program are presented in Table 1. Waves characterized by three wavelengths (7, 11, and 15 ft) were combined with phase shifts between adjacent wavemaker paddles. These phase shifts were approximately equivalent to the angle of the wavecrest with respect to the axis of the wave generator. The angle in the table shows the approximate correspondence between the phase lag and the angle of propagation.

Table 1
The Experimental Waves

Test Number	Wavelength (ft)	Phase Shift (deg)	Angle (deg)	Period (sec)
CN1007	7.0	10.0	7.45	1.378
CN1507	7.0	15.0	11.21	1.378
CN2007	7.0	20.0	15.03	1.378
CN3007	7.0	30.0	22.89	1.378
CN4007	7.0	40.0	31.23	1.378
CN1011	11.0	10.0	11.75	1.947
CN1511	11.0	15.0	17.79	1.947
CN2011	11.0	20.0	24.04	1.947
CN3011	11.0	30.0	37.67	1.947
CN1015	15.0	10.0	16.12	2.553
CN1515	15.0	15.0	24.62	2.553
CN2015	15.0	20.0	33.75	2.553

Genus 2 solutions can be visualized as a series of repeating two-dimensional permanent form surface patterns, referred to as period parallelograms. These patterns translate at a constant velocity in a constant direction. The global wave field is represented by a tiling of these basic patterns; therefore, the entire wave pattern can be exactly specified by quantifying just one period parallelogram. The location of a basic period parallelogram within the hexagonal wave field of Figure 2 is shown in Figure 4. The phase variables of Equation 5 define the horizontal limits of these patterns such that each side is uniquely defined by $\phi_1 = \text{constant}$ and $\phi_2 = \text{constant}$. The components of the Riemann matrix define the vertical and horizontal distribution within the period parallelogram.

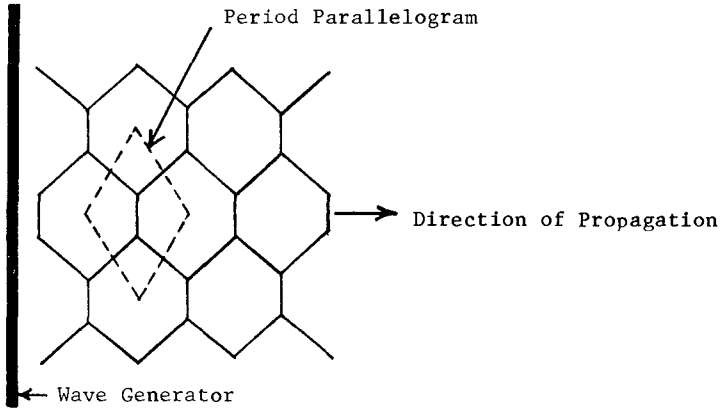


Figure 4. The Period Parallelogram

Detailed measurements of each of the generated wave fields shown in Table 1 were required in order to relate the physical characteristics of the waves to the parameters of the corresponding period parallelogram of the exact solution. This quantification was accomplished by first using overhead photography to determine the dimensions of the period parallelogram and to provide an estimate of the internal features, such as the phase shift and stem length. Knowledge of these horizontal features and their location within the wave tank were then used to locate a linear array of 9 recording wave gages in the wave basin. This approach provided a vertical wave record which could be identified with a known location within the parallelogram.

Comparing Theoretical Solutions To Observed Waves

The experimental program described above generates symmetric cnoidal waves ($\alpha_1 = \alpha_2$ in Figure 1) resulting in a symmetric period parallelogram. This simplification was adopted so that the generated wave patterns would propagate perpendicularly off the face of the wave generator, making it possible to measure all wave forms with a single stationary wave gage array. Symmetry also reduces the number of free parameters which need to be specified, for example, $\mu_1 = \mu_2$, $\nu_1 = -\nu_2$, and $\omega_1 = \omega_2$ from Equation 5. This simplification results in the requirement of only three dynamical parameters and two nondynamical parameters. The parameters chosen were b , μ , and λ along with the phase shift parameters ϕ_{10} and ϕ_{20} . The following sequence of events was used for optimizing these coefficients. Experiment CN3007 will be used to demonstrate the verification process.

Each of the waves of Table 1 were generated in the wave basin. Two overlapping photographs were taken with dual Hasselblad model 500EL/M 70mm cameras equipped with 50mm lenses mounted 23 ft above the floor of the basin. The resulting mosaic photograph, shown in Figure 5, was used to estimate the length and width of the period parallelogram. This resulted in estimates for $\mu_1 = \mu_2$ and $\nu_1 = -\nu_2$. An estimate for the phase shift parameter λ was also determined from the photograph. The accuracy of μ , ν , and λ is a function of the distortions in the photograph. Because of this distortion, their values were considered to be initial estimates. Following the photographing of all waves, a wave gage spacing of 2.5 ft apart and 40.0 ft from and parallel to the generator was selected for use in all tests. The location of each of the gages with respect to wave CN3007 is shown in Figure 5. It can be seen that each gage can be uniquely referenced according to a distance from the center of the parallelogram. Since all parallelograms are identical, wave gages located in an adjacent parallelogram can be referenced to the common center point.

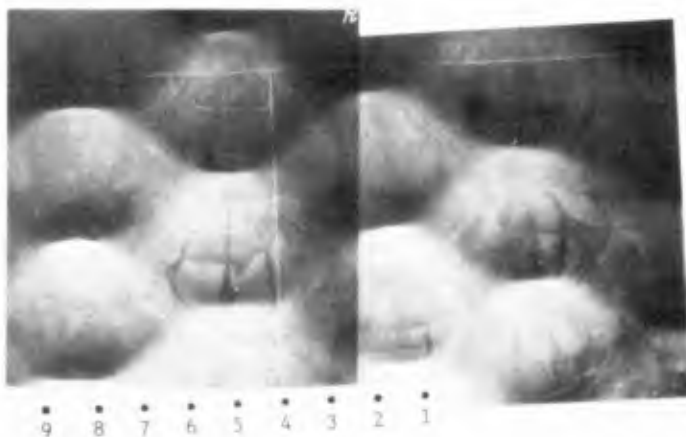


Figure 5. Overhead Mosaic Photograph of Test Wave CN3007

Wave gages were located in the basin and each of the waves of Table 1 were regenerated. Data was sampled for each of the gages at a rate of 50 samples per second for a total of 30.0 seconds. Figure 6 shows the wave traces for one period of wave CN3007. The correspondence between the wave traces and their location within the parallelogram can easily be seen. For example, gage 5 is located on a stem where only one peak per passing of the parallelogram is experienced. Gage 3 is located in the saddle region where two smaller peaks per period are seen. This comparison demonstrates the usefulness of the photographs in interpreting the data since three-dimensional effects are difficult to deduce from two-dimensional data.

CNOIDAL TEST CN3007

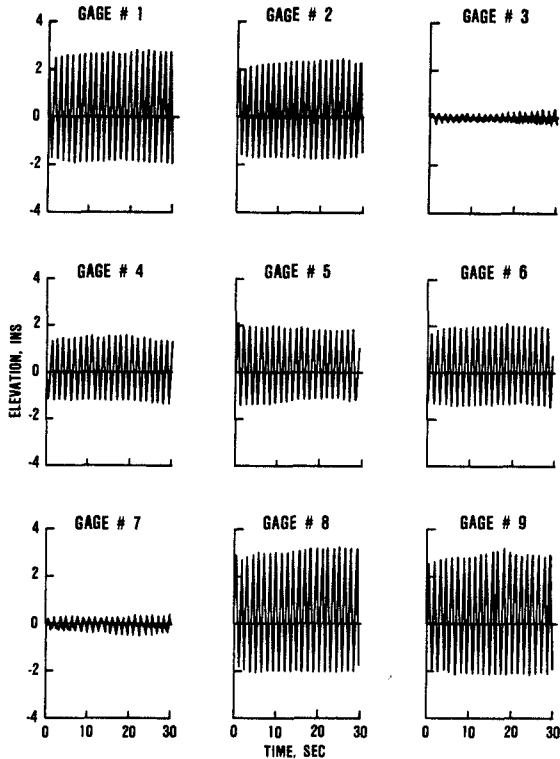


Figure 6. Wave Gage Traces for Test Wave CN3007

The determination of the free coefficients can now be made. Known or estimated data are the period of the wave (determined from the recording wave gages), the length and width of the period parallelogram and an estimate of the phase shift parameter λ determined from the photographs, and a maximum wave height selected from the wave gage data. The following iteration procedure was used to optimize the coefficients:

a. The estimated values for $\mu_1 = \mu_2$ and λ were specified. The nondynamical parameters ϕ_{10} and ϕ_{20} were accounted for by specifying solutions to be computed at location within the period parallelogram corresponding to the location of the wave gages. A value of b was then selected such that the dimensionalized maximum KP solution was within 5.0 percent of the measured value.

b. The value of $\mu_1 = \mu_2$ was adjusted, if necessary, until the dimensionalized period was within 3.0 percent of the measured period.

c. The value of λ was adjusted, if necessary, until the dimensionalized value of $v_1 = -v_2$ was within 10.0 percent of the estimated value. A 10-percent criteria was used for this iteration since the length of the parallelogram was difficult to determined from the photographs.

d. Because of the nonlinear coupling of the solution coefficients, each adjustment affected all parameters to some extent. If corrections were found to be necessary, steps (a.) through (c.) were repeated until all of the specified tolerances were

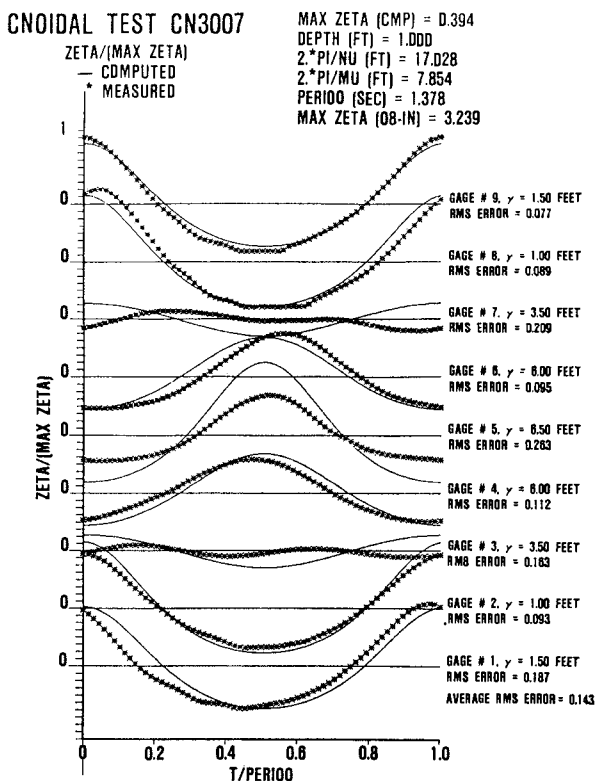


Figure 7. Theoretical and Measured Wave Profiles for Test Wave CN3007

met or exceeded. Possible phasing problems regarding the gage locations within the parallelogram were rectified by adjusting the nondynamical phase parameters.

e. A KP solution corresponding to the location of each of the wave gages was calculated. A normalized plot comparing theory to measurements was made, as shown in Figure 7 for the present example. Included in each plot is the Root Mean Square (RMS) error for each comparison.

f. A normalized contour plot (Figure 8) and a three-dimensional plot (Figure 9) for each wave field was finally prepared as a visual example of the KP solution.

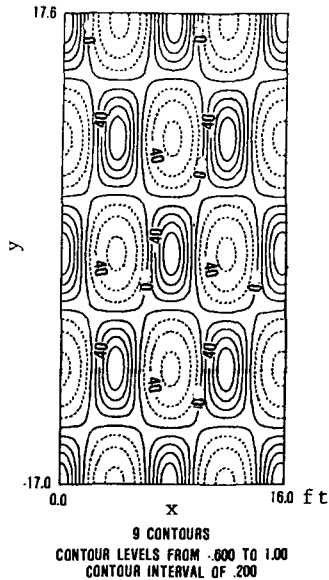


Figure 8. Normalized Contour Plot for Test Wave CN3007

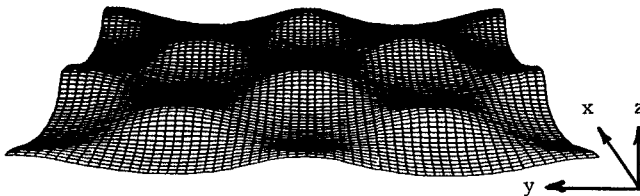


Figure 9. Three-Dimensional Plot of Test Wave CN3007

The above procedures were followed for each of the test wave fields of Table 1. A minimum tolerance of 5.0 percent for waveheight, 3.0 percent for period, and 10.0 percent for the Y-direction wavelength was maintained for all experiments. Table 2 presents those computed results. For each case, an average RMS error is provided which represents a simple average of the 9 RMS values computed for each gage. In no case did this error exceed 20 percent even though variations in the elevation of the basin floor of 10 percent were known to exist. Additionally, the experimental wave fields were generated almost to the point of breaking in order to span the range of solution parameters and investigate the limits of applicability of the genus 2 solutions. In view of these introduced and existing sources of potential error, the degree of fit between the generated wave fields and the exact solutions were found to be very good.

Table 2
Computed wave parameters

Test Number	Max. Height (in)	X-Wavelength (ft)	Y-Wavelength (ft)	Ave. RMS Error
CN1007	2.44	7.0	46.5	0.141
CN1507	3.59	7.2	35.1	0.188
CN2007	3.06	7.5	27.3	0.150
CN3007	3.24	7.9	17.0	0.143
CN4007	3.30	8.7	13.6	0.184
CN1011	2.23	10.7	48.0	0.174
CN1511	2.87	11.1	40.3	0.122
CN2011	3.10	11.6	27.6	0.126
CN3011	2.48	12.6	20.7	0.172
CN1015	2.65	15.0	59.3	0.120
CN1515	2.84	16.1	32.6	0.094
CN2015	2.86	17.1	29.0	0.098

Conclusions

Twelve separate nonlinear wave fields were generated for the purpose of verifying the KP equation to be an accurate model for three-dimensional nonlinear waves. Criteria were developed which provided a unique correspondence between the solution parameters of the KP equation and the physical characteristics of the laboratory generated waves. Results of these experiments showed that both the generated waves and the genus 2 solutions are remarkable robust in that both were stable over a wide range of parameters, including the near breaking of waves. The excellent degree of fit between the observed and computed solutions shows that genus 2 solutions of the KP equation represent a viable model for three-dimensional, nonlinear, shallow water waves.

Acknowledgments

The author is grateful to Drs. Harvey Segur and Joseph Hammack for their help and advice, both of which were necessary for the successful completion of this project. The research results contained in this paper were funded through a Department of the Army In-House Laboratory Independent Research (ILIR) program. The author wishes to acknowledge the Office, Chief of Engineers, U. S. Army Corps of Engineers, for authorizing publication of this paper.

References

- Dubrovin, B. A. (1981), "Theta Functions and Non-Linear Equations", Russian Math. Surveys, Vol. 36:2, pp 11-92.
- Hammack, J. L. (1980), Unpublished Experiments.
- Kadomtsev, B. B. and Petviashvili, V. I. (1970), "On the Stability of Solitary Waves in Weakly Dispersive Media", Soviet Physics - Doklady, Vol. 15, No. 6, pp 539-541.
- Korteweg, D. J. and deVries, G. (1895), "On the Change of Form of Long Waves Advancing in a Rectangular Channel, and on a New Type of Long Stationary Waves, Phil. Mag., Ser. 5, Vol. 39, pp 422-443.
- Segur, H. and Finkel, A. (1984), "An Analytical Model of Periodic Waves in Shallow Water", Aeronautical Research Associates of Princeton, Inc., Tech. Memo. 84-12.